LASER INTERFEROMETER GRAVITATIONAL WAVE OBSERVATORY
- LIGO -
CALIFORNIA INSTITUTE OF TECHNOLOGY
MASSACHUSETTS INSTITUTE OF TECHNOLOGY

Publication **LIGO-T980131-00 – D** 9/16/98

Simulation of the Alignment Sensitivity in LIGO Lock Acquisition

Marty Zwikel

Distribution of this draft:

all

This is a technical note of the LIGO Project.
(SURF Report)

LIGO Hanford Observatory
P.O. Box 1970 S9-02
Richland, WA 99352
Phone (509) 372-8106
FAX (509) 372-8137
E-mail: info@ligo.caltech.edu

LIGO Livingston Observatory
19100 LIGO Lane
Livingston, LA 70754
Phone (504) 686-3100
FAX (504) 686-7189
E-mail: info@ligo.caltech.edu

California Institute of Technology
LIGO Project - MS 51-33
Pasadena CA 91125
Phone (626) 395-2129
Fax (626) 304-9834
E-mail: info@ligo.caltech.edu

Massachusetts Institute of Technology
LIGO Project - MS NW17-161
Cambridge, MA 01239
Phone (617) 253-4824
Fax (617) 253-7014
E-mail: info@ligo.mit.edu

WWW: http://www.ligo.caltech.edu/

SIMULATION OF THE ALIGNMENT SENSITIVITY IN LIGO LOCK ACQUISITION

MARTY ZWIKEL
GRINNELL COLLEGE, GRINNELL, IA 50112

MENTOR: DANIEL SIGG
LIGO HANFORD OBSERVATORY, HANFORD, WA 99352

ABSTRACT

The laser interferometric gravitational-wave observatories (LIGOs) presently under construction in Hanford, WA and Livingston Parish, LA aim to detect a gravitational-wave strain on the order of 10^{-21}. To obtain this sensitivity, the interferometer must first be length locked on resonance. A scheme has been devised which sequentially locks the various LIGO cavities, but misalignments in the optical elements of these cavities reduce the signals used in lock acquisition. Of particular interest is the nominal "critical alignment," where length signals are degraded to half their aligned strengths. By simulating the LIGO lock signals for seismically driven mirror motions, we determine the critical alignment angles of the system. The final, and most sensitive, stages of lock acquisition are examined, with all possible misalignments of the optics expressed in a basis which is diagonal to signal sensitivity. We find a mirror speed independent critical alignment at 2×10^{-7} radians in the more sensitive angular degrees of freedom, while the other degrees have a lesser, but speed and stage dependent effect. The alignment signals and power readouts which will aid in lock acquisition are also examined, and are seen to remain useful at this critical alignment.

1. INTRODUCTION

Gravitational radiation is predicted to produce a quadrupolar strain in the space perpendicular to its direction of propagation [1]. For the LIGO-like (Laser Interferometric Gravitational-Wave Observatory) detectors being built today, gravity waves induce a differential length change in the orthogonal arms of such interferometers (see Fig. 1). The 4 kilometer Fabry-Perot cavities which will serve as the long-baseline arms for these detectors must be kept on resonance if gravitational-wave sensitivity is to be maintained. To achieve this condition for useful time spans, a length sensing and control (LSC) scheme was developed which yields correction signals proportional to cavity length deviation from resonance. These signals can then be used by a null servo system to dynamically correct the length error. In the configuration used by LIGO, four length degrees of freedom must be controlled for an overall length "lock" on cavity resonance [2]. A sequential locking procedure has been devised, which in practice will be known as "lock acquisition mode," to lead the interferometer into its gravitational-wave sensitive state, or "detection mode" [3].

Misalignments in the optical elements of the detector, however, may inhibit the lock acquisition process in all its stages. Angular deviations with respect to the incident laser beam can effectively increase shot noise at the detection ports, or decrease power build-up in the arm cavities (see Fig. 4). A total of ten angular degrees of freedom (five from each transverse dimension[1]) need to be controlled if the signals used to achieve length lock are to remain useful [4]. Unfortunately, the signals needed to correct misalignments cannot be produced without a nearly resonant interferometer. This makes the length and alignment control problem a "chicken-and-egg affair."

In this paper, we analyze the effects of misalignment on length lock acquisition. Using a dynamical model of the LIGO's field evolution, one can simulate the length and alignment signals in response to seismically driven mirror motions. First and foremost, we elucidate the length signal dependence on angular misalignment. We define critical alignment as the state for which length signals are reduced to half of their aligned strengths. The critical alignment of the interferometer is thus mapped out for the two final lock stages, predicted mirror speeds and angular degrees of freedom. Our most pronounced result is a mirror speed independent critical alignment at 2×10^{-7} rad in the more sensitive angular degrees of freedom, while the other degrees have a lesser, but speed and lock stage dependent effect. This suggests that the interferometer should first be aligned to this level in earlier stages of acquisition, prior to attempting a full lock of the entire system. We also examine the alignment signals which are available to correct angular deviations, and find that they are indeed usable when needed. Furthermore, alignment and cavity power buildup are described in their angle and speed dependence, as these might be secondary tools used in lock acquisition.

[1] There are six mirrors in the LIGO configuration, but any beamsplitter misalignment can always be viewed as a misalignment of the perpendicular arm. Thus there are five angular degrees of freedom for each transverse dimension.

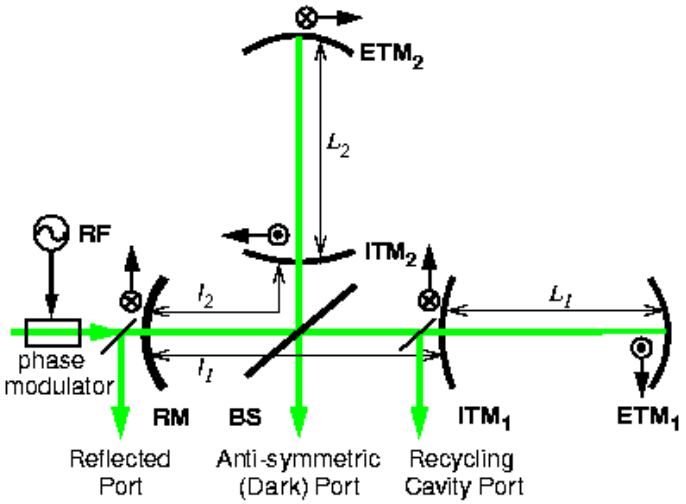

Figure 1: Schematic of the basic LIGO configuration. All four length degrees of freedom (l_1, l_2, L_1, L_2) and five angular degrees of freedom (ITM_1, ETM_1, ITM_2, ETM_2, RM) are shown above, along with the three length and alignment detection ports. Note that ITM, ETM and RM stand for input test mass, end test mass and recycling mirror, respectively.

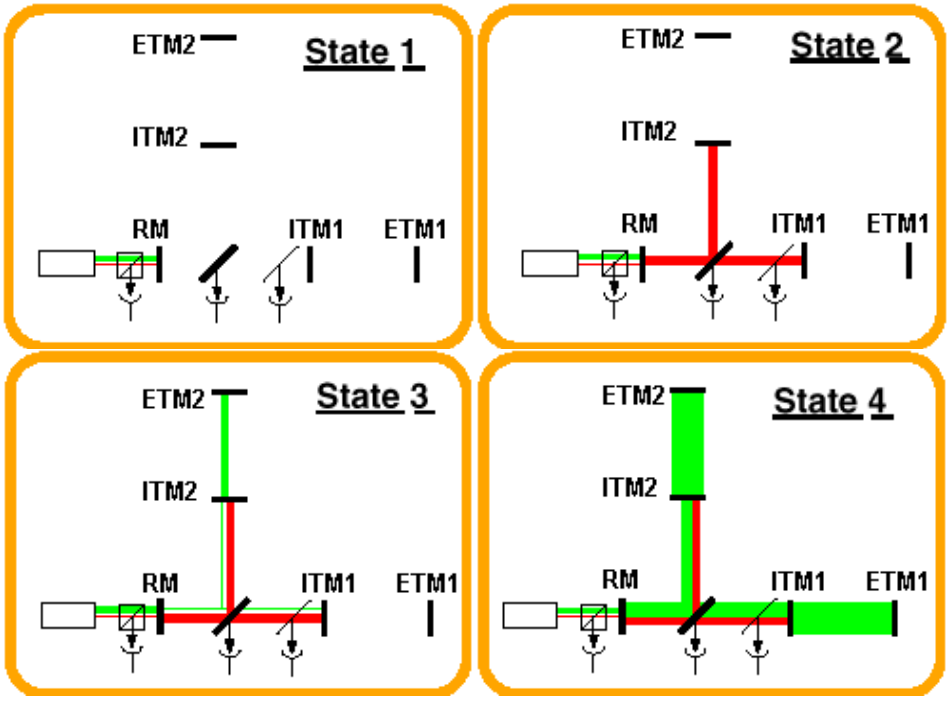

Figure 2: Length lock acquisition. At first, LIGO's mirrors all float freely (State 1). The sidebands are then locked to the recycling cavity (State 2), and at the same time the carrier is put on a dark fringe in the small Michelson. We next lock one arm to the carrier frequency (State 3), and acquire control over three length degrees of freedom. Finally, the last arm is locked, and the entire interferometer becomes resonant.

2. SIMULATION PROCEDURE AND METHODOLOGY

Simulations were conducted using the *IFO* code written by R. Beausoleil. This program evolves the LIGO electric fields, decomposed in Hermite-Gaussian modes, in time [5]. We use this code, via *Mathlink*, from a *Mathematica* front-end. For our purposes, *IFO* accepts as input parameters the mechanical state of the interferometer (mirror positions, speeds, and angular orientation) at a certain start time, and then iteratively calculates and updates the interferometer's response over a user defined time domain. The output is a time series of all the length, alignment and power signals the actual LIGO will produce, along with some "fictional" detectors for debugging purposes.

All of the simulations conducted for this work are, of course, based around the LIGO lock acquisition scheme (see Fig. 2). Since only the last two stages of acquisition are considered 'difficult,' we will neglect stages one and two in our simulations. In length, transitions three and four involve moving one of the six mirrors; ETM2 in the case of stage three, and ETM1 for stage four. We scan these mirrors, at a constant velocity, over a very small portion of a wavelength, with the exact point of resonance always being at the middle of our time trace. Microseismic driving forces are expected to induce mirror motions on the order of 1μm/s in velocity, but for completeness and comparison with the more well known steady state regime, we consider a wide spread of velocities from 0.001 to 10 μm/s [6].

The issue of which angular degrees of freedom to examine and what misalignment magnitude to test is somewhat more complicated. We wish to cover all possible misalignments, but working with the individual mirrors is not the most appropriate choice in angle bases for a number of reasons. For one, the wavefront sensors used to obtain alignment signals are most sensitive to the nominal *u-basis*:

$$\begin{bmatrix} \mathrm{U1} \\ \mathrm{U2} \\ \mathrm{U3} \\ \mathrm{U4} \\ \mathrm{U5} \end{bmatrix} = \begin{bmatrix} 0 & 0 & 0 & -0.58 & 0.81 \\ 0.91 & 0.42 & 0 & 0 & 0 \\ -0.42 & 0.91 & 0 & 0 & 0 \\ 0 & 0 & 0.92 & 0.32 & 0.23 \\ 0 & 0 & -0.39 & 0.75 & 0.54 \end{bmatrix} \begin{bmatrix} \Delta\mathrm{ETM} \\ \Delta\mathrm{ITM} \\ \overline{\mathrm{ETM}} \\ \overline{\mathrm{ITM}} \\ \mathrm{RM} \end{bmatrix}, \tag{1}$$

where,

$$\begin{bmatrix} \Delta\mathrm{ETM} \\ \Delta\mathrm{ITM} \\ \overline{\mathrm{ETM}} \\ \overline{\mathrm{ITM}} \\ \mathrm{RM} \end{bmatrix} = \frac{1}{\sqrt{2}} \begin{bmatrix} 0 & -1 & 0 & 1 & 0 \\ -1 & 0 & 1 & 0 & 0 \\ 0 & 1 & 0 & 1 & 0 \\ 1 & 0 & 1 & 0 & 0 \\ 0 & 0 & 0 & 0 & \sqrt{2} \end{bmatrix} \begin{bmatrix} \mathrm{ITM1} \\ \mathrm{ETM1} \\ \mathrm{ITM2} \\ \mathrm{ETM2} \\ \mathrm{RM} \end{bmatrix} \tag{2}$$

is the common & differential basis. As described in Fritschel *et al*., the *u-basis* is diagonal to, and ordered by, gravitational-wave sensitivity [7]. Essentially this means that misalignments in the U1 degree of freedom lead to the most degradation of gravitational-wave signal, while a U5 misalignment would be relatively inconsequential.

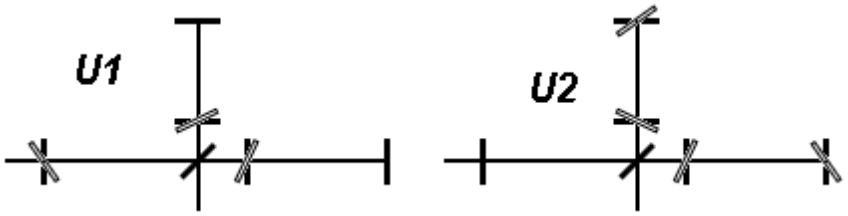

Figure 3: Examples of the most sensitive degrees of freedom in the U-Basis.

By simulating misalignments in the *u-basis*, only two degrees of freedom need be scrutinized. We need not focus on misalignments in U3, U4, or U5, as these combinations are known to produce little signal degradation.

In stage three, where we attempt to lock a single arm cavity, one is more concerned with the production of sideband TEM_{10} mode. The power recycling cavity, due to its short length, is highly degenerate for its resonant sideband field, and is thus inherently more sensitive to misalignments. Misalignments effectively reduce the power at the fundamental frequency, and thereby degrade the length signals which would be used in this stage[2]. As shown in Fig. 3, the U1 angle from our earlier basis deals only with the recycling cavity. This combination is therefore most critical for length sensing and control, so we place it, as M1, at the forefront of the *m-basis*, our choice for stage three:

$$\begin{bmatrix} \text{M1} \\ \text{M2} \\ \text{M3} \\ \text{M4} \\ \text{M5} \end{bmatrix} = \frac{1}{\sqrt{2}} \begin{bmatrix} 0.580 & 0 & 0.580 & 0 & -1.146 \\ 0.813 & 0 & 0.813 & 0 & 0.823 \\ -1 & 0 & 1 & 0 & 0 \\ 0 & \sqrt{2} & 0 & 0 & 0 \\ 0 & 0 & 0 & \sqrt{2} & 0 \end{bmatrix} \begin{bmatrix} \text{ITM1} \\ \text{ETM1} \\ \text{ITM2} \\ \text{ETM2} \\ \text{RM} \end{bmatrix} \tag{3}$$

The remainder of this basis is essentially arbitrary – all that we require is unitarity and orthogonality. It should be noted that M2, which was specifically constructed to be orthogonal to M1, is its tolerant (*i.e.*, least TEM_{10} producing) counterpart. With these bases now constructed for their particular stages, we have defined all of our simulation parameters and their ranges – the full spectrum of simulator input.

As mentioned earlier, Beausoleil's *IFO* outputs a large array of LIGO error signals. In analyzing the effects of misalignment on lock acquisition, however, only a few of these detection ports are interesting. Specifically, we are concerned with the length sensors at the pick-off and dark port for stages three and four, respectively [1]. In alignment, we examine only the wavefront sensors which detect U1 (or M1) and U2 misalignments. As for power signals, in stage four we focus on the arm cavity carrier build-up, while in stage three we look at the resonant sideband power in the recycling cavity. Both of these power readings are intimately related to length signal sensitivity.

[2] The carrier fundamental acquires an additional phase of π on reflection from the arms, while it's higher order modes do not. For this reason, the recycling cavity is *not* degenerate at the carrier frequency.

3. RESULTS

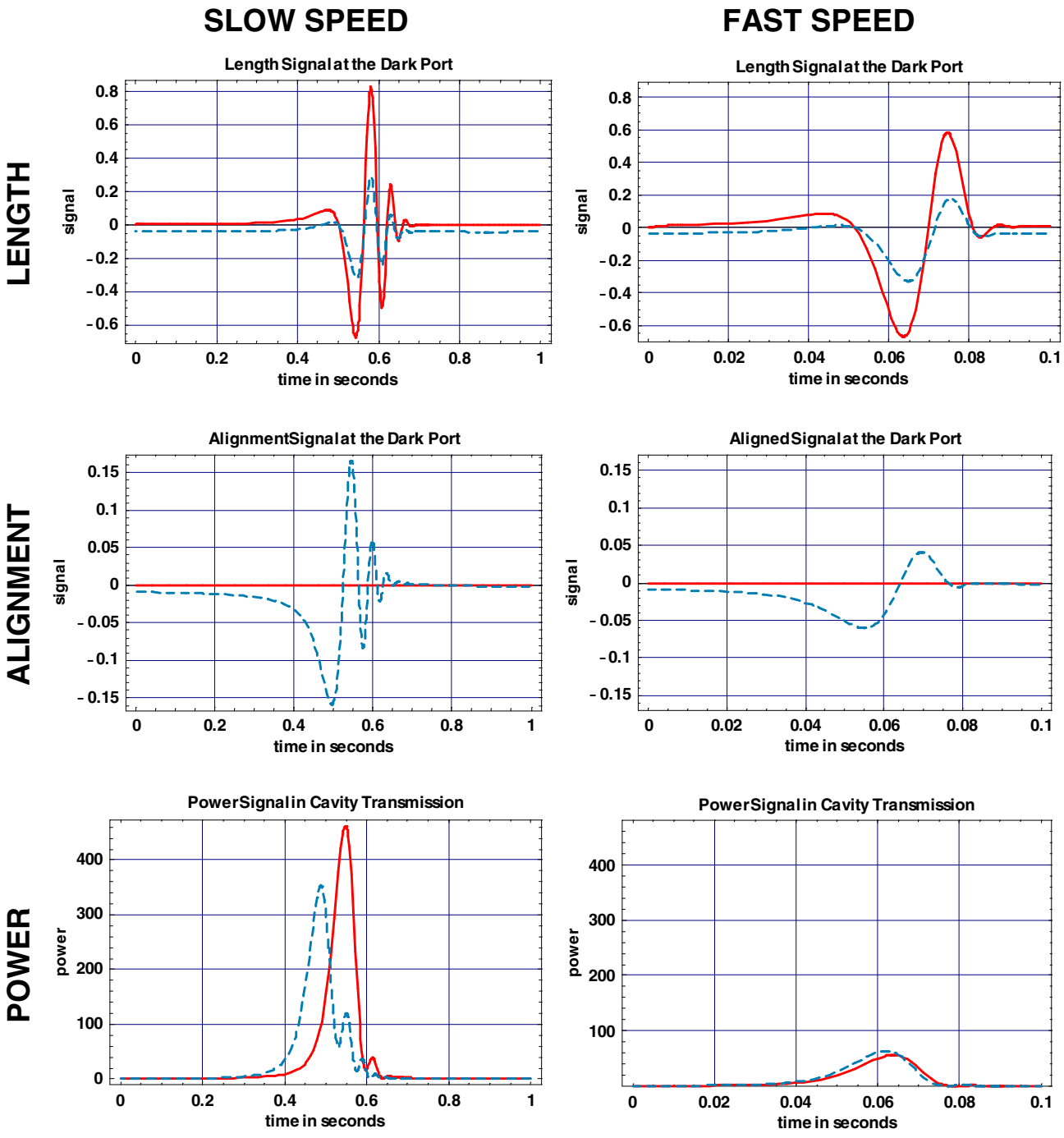

Figure 4: Sample detector output signals. All three signal types are given, along with two scan speeds: nominal slow (0.005 μm/s) and nominal fast (0.05 μm/s). While 0.05 μm/s is not "fast" given the entire range of speeds simulated, it facilitates the same-scale comparisons provided above. Within each plot, we have an aligned system (solid curve) and a 0.02 divergence half angle misalignment (dashed curve). Note that the length signals have U1 misalignments, while alignment and power are shown with U2 misalignments. All scans were produced in stage four lock acquisition.

At each mirror speed, we simulate all angular degrees of freedom for a spread in misalignments ranging from 0.01 of the arm cavity divergence half angle (θ_D=9.65×10^{-6} radians) to 0.2, at which point more transverse modes (and computation time) would be required.

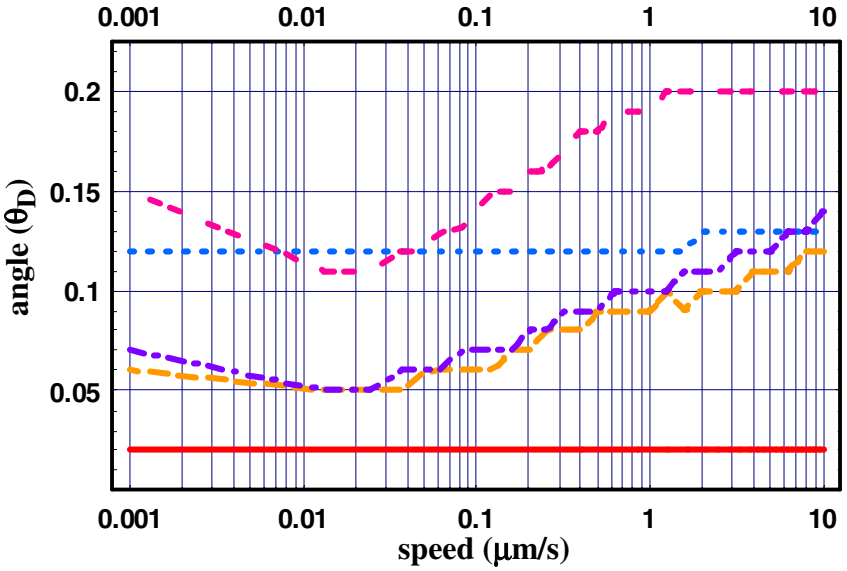

Figure 5: Stage four critical alignment. Angles at which the dark port length signal drops to half of its aligned value. Results are given for U1 (solid curve), U2 (dashed), U3 (dotted), U4 (dash-dot), U5 (dash-dash).

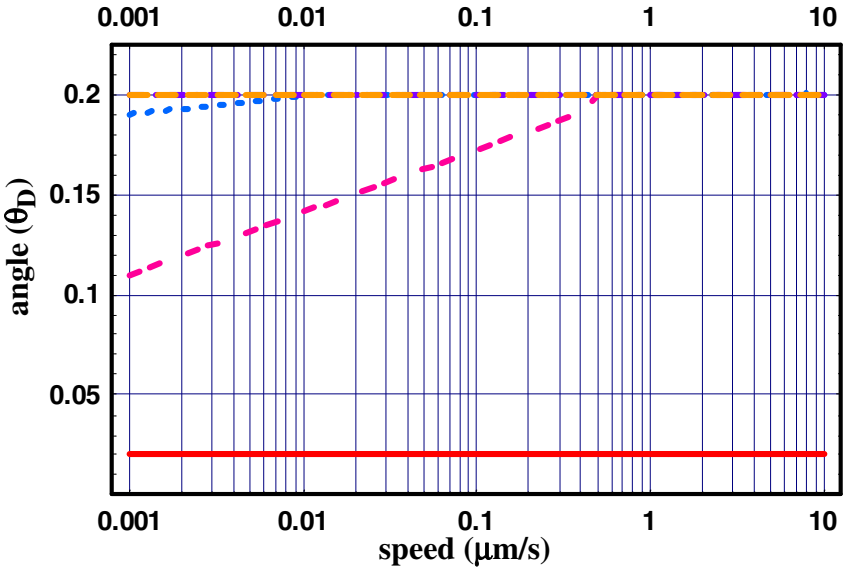

Figure 6: Stage three critical alignment. Angles at which the pick-off port length signal drops to half its aligned value. Results are given for M1 (solid curve), M2 (dashed), M3 (dotted), M4 (dash-dot), M5 (dash-dash). Note that the M2 and M4 curves are simply constant angles of 0.2 θ_D.

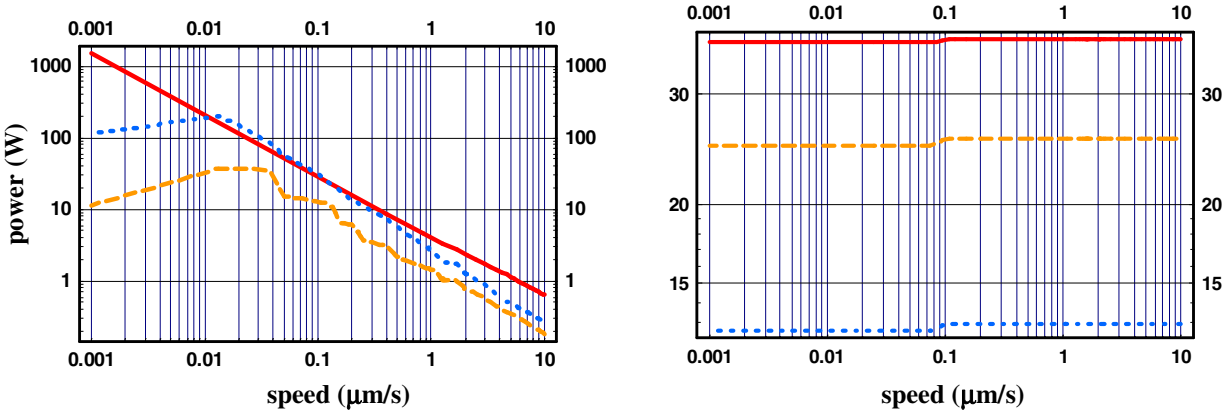

Figure 7: Stage four power for U2 misalignments (left). Maximum cavity power of the in-line arm cavity as it is affected by arm cavity misalignments. Aligned (solid curve), 75% critical (dotted), critical alignment (dashed). Note that for U1 misalignments up to and over the critical angle, arm cavity (carrier) power is essentially unaffected, and could be regarded as the aligned (solid) curve of this plot as well.

Figure 8: Stage three power for M1 misalignments (right). Resonant sideband power in the recycling cavity, as it is affected by misalignments in this cavity. Aligned (solid curve), 75% critical in M1 (dashed), critical alignment (dotted).

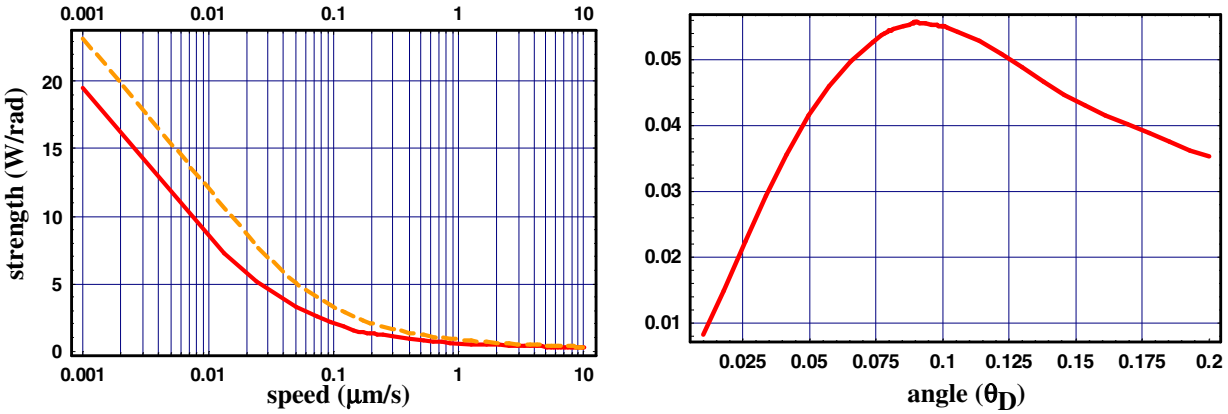

Figure 9: Stage four alignment signal at 0.02 θ_D. An illustration of the speed dependence of wavefront sensor signals for U1 (solid curve) and U2 (dashed) at a constant misalignment. Note that the U1 curve, which is read from the pick-off port, has been scaled by a factor of 50 for comparison with U2's signals, which are read from the dark port.

Figure 10: U2 alignment signal angle dependence. Arm cavity misalignment response for stage four, constructed at a mirror speed of 1.0 μm/s.

4. DISCUSSION

Our discussion of the simulation results from previous pages will focus largely on the final stage of lock acquisition, stage four. The sample detector output signals shown in Fig. 4 were all taken from this stage, and will be referred to a number of times in this discussion. However, let us begin with a short comparison of stages three and four in order to justify this bias. As is evident by comparison of Figures 5 and 6, the critical alignment environment of stage four is far more complicated than that of stage three. An obvious speed dependence exists in three out of five degrees for stage four, whereas stage three critical alignment angles are by and large speed independent. Except for the linear behavior of M5 at slow speeds, which for lock acquisition are practically unimportant, all but one degree of freedom have huge critical alignment angles, indicating that misalignment has little effect on length sensing in this stage. The one remaining degree of freedom, M1 (or U1), induces critical alignment for a relatively small misalignment of 2×10^{-7} radians, and does so in both stages. With regard to stage three, this is just as predicted – M1 was the cornerstone of our angle basis for this stage. That this degree poses such a problem in stage four acquisition as well can be taken as a mandate to first align and lock the recycling cavity, the U1 angular domain, before proceeding to the arm cavities. With this done, stage three acquisition becomes significantly easier from the perspective of alignment sensitivity. This fact warrants our paying full attention to the more complicated stage four, which we turn to next.

As in stage three, misalignments in the U1 angle form a sort of critical alignment wall at 2×10^{-7} radians, but assuming this is dealt with in earlier stages of acquisition, we may focus on the other angular degrees of freedom. The median mirror speed prediction at the LIGO Hanford observatory is on the order of 1 μm/s, so let us confine our remarks to velocities from 0.1 to 10 μm/s for the time being. In this range, critical alignment angles in U2, U4 and U5 steadily increase with speed. This is purely an arm cavity issue: fast mirror speeds allow for little power build-up to begin with, and misalignments become only a second order effect in reducing this build-up. We thus have a factor of three to five times more tolerance to misalignments than the U1 lower bound.

There is a down-side to these other degrees of freedom, however, in that arm cavity misalignments directly affect the carrier power build-up where it is needed most (see Fig. 7). Even an aligned interferometer has power fall-off that is directly proportional to mirror speed. At critical alignment in U2, the most sensitive of the arm cavity degrees of freedom, power build-up is reduced by half an order of magnitude in the fast speed range. For slow speeds, where alignment is the first order variable, losses are around two orders. Even at 75% critical alignment, we still lose a full order; indicating that power loss is a strong function of this misalignment.

By constrast, U1 misalignments have very nearly zero effect on arm cavity power. This is of course due to U1's dependence on the sideband power build-up in the recycling cavity. Thus, while our length signals are highly sensitive to this degree of freedom, power can provide some sort of backup in lock acquisition. Recycling cavity power, specifically sideband power, is another story altogether, as shown in Figure 8. The most obvious fact of this plot is that resonant sideband power has virtually no speed dependence. In practice and in modeling, the recycling cavity length is on the order of meters, and therefore all relative mirror speeds examined herein are extremely slow from

its perspective. In alignment, however, we have a strong dependence. The aligned power of 36 Watts is reduced to 25 Watts at 50% critical alignment (*i.e.*, 10^{-7} radians), and to 13 Watts at 2×10^{-7} radians. It is *this* power signal then which is a strong function of U1; in fact critical alignment in length is roughly equivalent to critical alignment in power.

Now that we've seen how these two signals types, length and power, respond to misalignments, let's examine the alignment signals themselves. Even though lock acquisition seems manageable from a length and power perspective, we must still be able to re-align when necessary. Figure 9 illustrates the speed dependence of LIGO's wavefront sensors. Signal strength for both recycling (U1) and arm cavity (U2) misalignments goes like a power law with speed. An examination of the sample alignment signals provided (see Fig. 4) shows just how dramatic this drop off is. Nonetheless, the sensors still peak at the point of resonance, which in principle provides us with another source of length information. Speculations as to the servo mechanism which might utilize all this information are beyond the scope of this paper, but it should be noted that even at critical alignment in length, alignment signals are useful in and of themselves for length lock acquisition.

One might now begin to wonder about a measure of critical alignment in wavefront sensing. By plotting these sensor strengths as a function of misalignment angle, we can see where the wavefront sensors lose their usefulness for both length and angular corrections. Theory predicts that the response to angular deviations ought be linear up to a certain angle, as shown in Figure 11 [8]. Comparison of this plot with the experimental Figure 10 shows them to be in good agreement. In these cases, we are considering a differential (U2) misalignment at the very reasonable speed of 1μm/s. If one is to use the same "half maximum" criteria, critical alignment in wavefront sensing occurs near 1.2×10^{-6} radians, twice the critical angle in length for this degree of freedom[3].

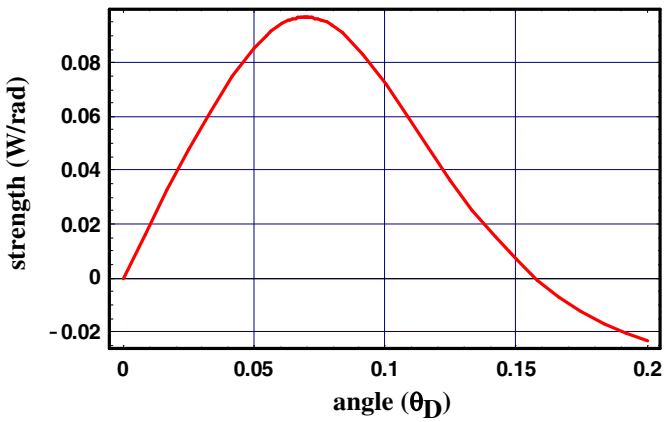

Figure 11: Theoretical alignment response. Results are given for a single cavity with differential misalignments on the scale of Figure 10. Four modes were used in this calculation.

[3] The careful reader will notice that I am using the theoretical plot from Figure 11 in making this statement, even though the experimental data indicates a better critical alignment. I choose the conservative angle because running simulations with higher order modes would curb the alignment peak much more rapidly.

5. CONCLUSIONS

In this work we have assessed the effects of angular misalignment on the LIGO length lock acquisition scheme. The critical alignment conditions for each of the final two stages of this procedure have been presented for constant mirror speed. Essentially, a recycling cavity misalignment of 2×10^{-7} radians stands as the lower bound on misalignment for all stages of length locking. Assuming this requirement is dealt with first, differential arm cavity misalignments lead to the most degradation of length signals in stage four of acquisition, while stage three can be regarded as significantly less sensitive.

Examination of the power and alignment signals available during locking has shown them to remain useful for the most sensitive mirror misalignments, even at relatively high speeds. In the case of recycling cavity misalignments, arm cavity power provides a backup tool in resonance finding. Arm cavity misalignments, however, strongly affect arm cavity power build-up, but length signals are more tolerant to these angular degrees of freedom anyway. In wavefront sensing, signals stay usable for somewhat higher angles, making them useful not only in alignment correction, but also as an independent tool for length locking.

The code used for these simulations may, in the near future, be used to investigate the more involved problem of designing a servo system that can control all length and angular degrees of freedom. As the LIGO interferometers begin to come on-line, the tolerances and sensitivities assessed in this work will serve as useful tools in understanding their behavior during initial phases of operation.

ACKNOWLEDGEMENTS

The author would like to thank Daniel Sigg for his patient explanation of the theory behind the LIGO length and alignment issue, his many suggestions and contributions toward running these simulations, his aid and assistance in interpreting the results, and his Michelango-brand lasagna which will soon be repaid. Much appreciation goes to Ray Beausoleil as well for providing the simulation code used throughout this project.

REFERENCES

[1] K.S. Thorne, "*Gravitational radiation*," in *300 Years of Gravitation*, S.W. Hawking and W. Israel, eds. (Cambridge U. Press, Cambridge, 1987), Chap. 9, pp. 330-458.

[2] M.W. Regehr, F.J. Raab, and S.E. Whitcomb, "*Demonstration of a power-recycled Michelson interferometer with Fabry-Perot arms by frontal modulation*," Appl. Opt. **20**, 1507-1509 (1995).

[3] P. Fritschel, G. Gonzalez, A. Marin, N. Mavalvala, D. Ouimette, L. Sievers, D. Sigg, and M. Zucker, "*Length Sensing and Control System Preliminary Design*," LIGO Technical Note, LIGO-T9700122-00-D (1997).

[4] N. Mavalvala, D. Sigg, and D. Shoemaker, "*Experimental Test of an Alignment Sensing Scheme for a Gravitational-wave Interferometer*," *accepted by Applied Optics*.

[5] R.G. Beausoleil, "*Spatiotemporal Model of the LIGO Interferometer*," *private communication* (1998).

[6] F. Raab and D. Coyne, "*Effect of Microseismic Noise on a LIGO Interferometer*," LIGO Technical Note, LIGO-T960187-01-D (1997).

[7] P. Fritschel, G. Gonzalez, N. Mavalvala, D. Shoemaker, D. Sigg, and M. Zucker, "*Alignment of an Interferometric Gravitational-wave Detector*," *accepted by Applied Optics*.

[8] Y. Hefetz, N. Mavalvala, and D. Sigg, "*Principles of calculating alignment signals in complex resonant optical interferometers*," J. Opt. Soc. Am. B. **14**, 1597-1605 (1997).